Current Biology, Vol. 14, 2113–2118, December 14, 2004, ©2004 Elsevier Ltd. All rights reserved. DOI 10.1016/j.cub.2004.11.028

Effects of Imposed Bending on Microtubule Sliding in Sperm Flagella

Yutaka Morita[1] and Chikako Shingyoji*
Department of Biological Sciences
Graduate School of Science
University of Tokyo
Hongo, Tokyo 113-0033
Japan

Summary

The movement of eukaryotic flagella is characterized by its oscillatory nature [1]. In sea urchin sperm, for example, planar bends are formed in alternating directions at the base of the flagellum and travel toward the tip as continuous waves. The bending is caused by the orchestrated activity of dynein arms to induce patterned sliding between doublet microtubules of the flagellar axoneme. Although the mechanism regulating the dynein activity is unknown, previous studies [2–7] have suggested that the flagellar bending itself is important in the feedback mechanism responsible for the oscillatory bending. If so, experimentally bending the microtubules would be expected to affect the sliding activity of dynein. Here we report on experiments with bundles of doublets obtained by inducing sliding in elastase-treated axonemes [8]. Our results show that bending not only "switches" the dynein activity on and off but also affects the microtubule sliding velocity, thus supporting the idea that bending is involved in the self-regulatory mechanism underlying flagellar oscillation.

Results and Discussion

Elastase-treated axonemes of sea urchin sperm flagella have characteristics that make them suitable for studying the effect of bending on microtubule sliding. Unlike the more conventional trypsin-treated axonemes, which on exposure to ATP disintegrate into individual doublets as the result of microtubule sliding, elastase-treated axonemes split lengthwise into two bundles of doublets by sliding at limited interdoublet sites unless the concentration of ATP is <0.1 mM, when they disintegrate into individual doublet microtubules [8–10]. In addition, the elastase-treated axonemes are capable of cyclical bending in response to repetitive local application of ATP [11]. These characteristics seem to indicate that the elastase-treated axonemes retain the structure involved in the regulation of microtubule sliding to form bends [8, 11].

We induced sliding disintegration of elastase-treated axonemes by releasing ATP with a 60 ms UV flash in an assay buffer containing 0.5 mM caged ATP [12] and 10^{-4} M Ca^{2+}. Under these conditions, about 25% of the axonemes showed microtubule sliding, which in most (90%) of the cases split the axoneme into two unequally thick microtubule bundles that slid for some distance along each other (Figure 1A). By repeating the UV flashes, we could induce sliding between the pair of bundles several times (Figure 1A). Because the separation of the axoneme into two doublet bundles was similar to that induced by 1 mM ATP in our previous study [8], we assumed that the thicker of the bundles observed in this study contained the central pair microtubules (CP) as well as five or six doublets, whereas the thinner bundle contained the remaining four or three doublets but no CP.

We then bent a part of either the thinner or the thicker bundle of a partially overlapping pair with a glass microneedle. Photoreleasing ATP induced further sliding between the two bundles in about 60% of these bent axonemes (Figure 1B; second and third black bars in Figure 1D); the remaining 40% disintegrated into many small bundles or individual doublets (Figure 1C; second and third white bars in Figure 1D). Without bending (Figure 1D, top bar), most of the axonemes (90%) showed sliding only between the existing two bundles (black bar), with only 10% disintegrating into individual doublets (white bar). Bending the region of overlap between the thinner and thicker bundles also induced a similar increase in the proportion of paired bundles that disintegrated into many bundles or individual doublets (bottom bar in Figure 1D). In axonemes from which the outer arms had been removed, bending also increased the occurrence of sliding disintegration into many small bundles (Figure 1E, white bars). These results indicate that bending activated those dynein arms that were otherwise inactive in the bundle and that the effect was independent of the presence or absence of the outer arms.

We have previously shown [8] that the dynein arms on the thinner bundle, but not those on the thicker bundle, are mainly active to induce the separation of elastase-treated axonemes. Because dynein arms are minus end-directed motor proteins [13, 14], they move the adjacent doublet bundle toward its plus end. Therefore, if the dynein arms on the thicker bundle become active instead of those on the thinner bundle, the direction of movement of the bundles relative to each other would reverse. This did not occur in unbent bundles; the two bundles in each pair continued to move in the same relative directions upon several UV flashes (Table 1, without bending; Figures $2A_{1–3}$ and $2B_{1–3}$).

When the region of overlap between the two bundles was bent with a microneedle, however, subsequent application of ATP induced "backward" sliding in 45% of the pairs (Figures $2A_{3–5}$ and $2B_{3–6}$; Table 1). That is, the direction of relative movement of the bundles was reversed by the bending. It is probable that the dynein arms on the thicker bundle, instead of those on the thinner bundle, became active by bending. Bending the nonoverlapping regions of the thinner or thicker bundles could also induce reverse sliding, although at much lower frequencies (6% and 14%, respectively) than that

*Correspondence: chikako@biol.s.u-tokyo.ac.jp
[1]Present address: Department of Biomolecular and Integrated Medical Sciences, Graduate School of Comprehensive Human Sciences, University of Tsukuba, Ibaraki, Japan.

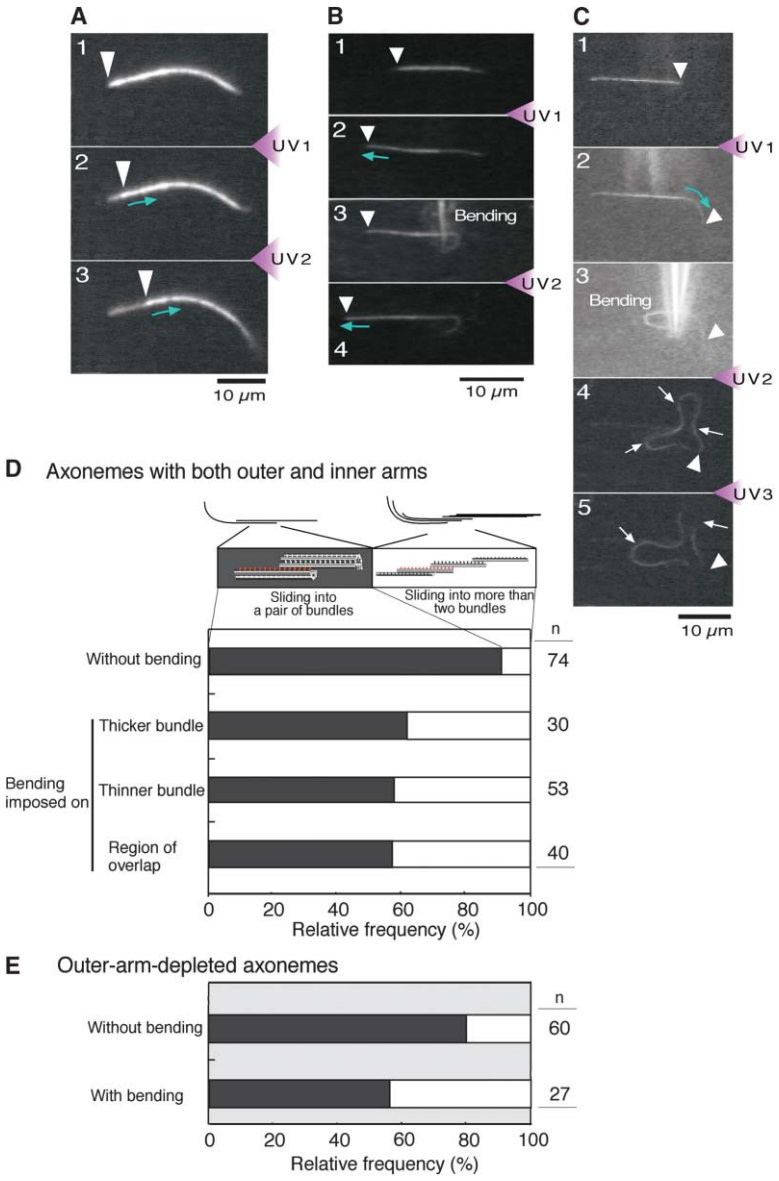

Figure 1. Sliding in Elastase-Treated Axonemes with or without Bending

Video images showing sliding in elastase-treated axonemes (A–C). Arrowheads indicate the left (A and B) or the right (C) edge of the thinner (A and C) or the thicker (B) bundles that were sliding. The first (in [A]–[C]) and second (in [A]) UV flashes induced sliding that separated the axoneme into two bundles (arrows in color). After bending the bundle with a microneedle (B_3 and C_3), the second flash induced further sliding of the thicker bundle in the same direction as before (B_4; arrow in color), and the second and third flashes induced sliding into more than two bundles ($C_{4 \text{ and } 5}$; white arrows). The effect of bending on sliding patterns was observed after the second UV flash with or without bending in "both-arms-intact" (D) and outer arm-depleted axonemes (E). In bent bundles, fewer bundles showed sliding between the pair of doublet bundles (black bars), and more bundles were separated by sliding into individual doublets (white bars) than in unbent bundles.

of the backward sliding induced by bending the region of overlap.

For inducing backward sliding, bending the bundle by more than about 90 degrees was effective. Although the effect was observed by bending up to about 180 degrees, quantitative analysis of the effect of bending angle on the backward sliding was not done because of technical difficulties. Neither was the effect of the curvature quantitatively analyzed. In some experiments the bundle that was being bent by the microneedle became detached from the latter during the backward sliding induced by a UV flash. The detached bundle tended to straighten, apparently by elastic recoil. Interestingly, subsequent applications of ATP to such bundles with greatly reduced curvature induced backward sliding, provided the bending angle at the first UV flash was larger than about 90 degrees (Figure $2B_{5-6}$). It is likely that the bending is needed only for "switching" the activity of dynein arms [8, 15–18] from one bundle to the other.

It was not always the case that the bundle that was bent was the one that moved backward. This indicates that the bundles that slid backward were not passively

Table 1. Effects of Bending on the Direction of Sliding in Elastase-Treated Axonemes

Regions Bent	Number of Axonemes	Direction of Sliding	
		Normal	Reverse
Thicker Bundle	21 (100%)	18 (86%)	3 (14%)*
Thinner Bundle	33 (100%)	31 (94%)	2 (6%)*
Overlap	42 (100%)	23 (55%)	19 (45%)*
Bending Total	96 (100%)	72 (75%)	24 (25%)
Without Bending	67 (100%)	67 (100%)	0 (0%)

Asterisks indicate that reverse sliding occurs significantly more frequently when the region of overlap of the two bundles was bent than when the region consisting of the thinner or thicker bundle alone was bent (χ^2 test, $p < 0.001$).

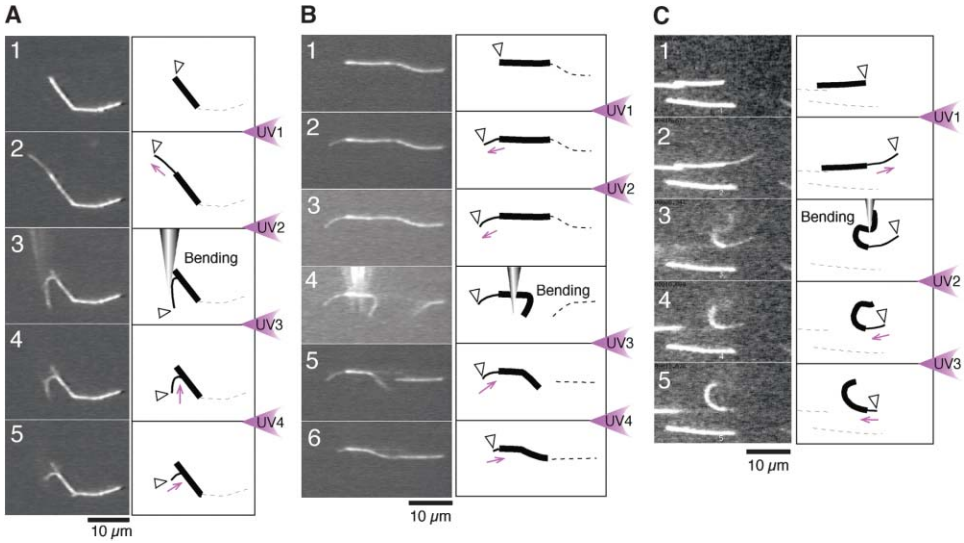

Figure 2. Effects of Bending the Doublet Bundle on the Direction of Sliding

Video images (left panels) with explanatory diagrams (right panels) showing axonemes with both the outer and inner dynein arms intact (A and B) and outer arm-depleted axonemes (C). Arrowheads indicate the left (A and B) or the right (C) edge of the thinner bundles, which slid out from the axonemes before the bending and then slid back after the region of overlap between the bundles was bent. The phase-contrast images of the microneedle were recorded over the fluorescent images (A_3 and B_4).

pushed back by the microneedle. Backward sliding of bundles was also induced in outer arm-depleted axonemes (Figure 2C), although at a very low frequency even when the region of overlap was bent (5%, n = 41). Because the treatment with 0.75 M KCl removed about 30% of the inner dynein arms as well as the outer arms [10], it is possible that these inner arms play a role in the backward sliding. The 0.75 M KCl-treated axonemes did not beat when ATP was applied in the bath, indicating that the switching mechanism necessary for producing bidirectional bends is destroyed by the high-salt treatment. Taken together, these results indicate that the backward sliding reflects the function of the switching mechanism that underlies the normal oscillatory movement of flagella.

We also found that bending increased the velocity of sliding. The sliding velocity (SV) in the elastase-treated axonemes that split into two bundles after a UV flash was about 2 μm/s, which changed little upon successive UV flashes. Thus, in the axonemes that were not bent by the microneedle, the ratio of the SV on the second flash to that on the first flash was 0.83 ± 0.29 (n = 19; mean ± the standard deviation). If the bundle was bent after the first sliding and then given a second UV flash, this ratio (SV of normally directed sliding after the second flash with bending/SV after the first flash without bending) became 1.52 ± 0.81 (n = 20). The increase was statistically significant ($p < 0.005$, Mann-Whitney U test). A similar increase of the sliding velocity was also observed in the backward sliding. In the outer arm-depleted axonemes, however, the ratio of the SV with bending (1.15 ± 0.48; n = 18) was not different from the SV without bending (1.17 ± 0.64; n = 18). These results are consistent with the previous works indicating that the outer arms play an important role in increasing the velocity of microtubule sliding in beating flagella [10, 19–21].

Previous studies have shown that over the physiological range of ATP concentrations, the main sliding takes place by the activity of dynein arms on the doublet microtubules #7 and #3 (or #4), which are situated along either side of the CP (Figure 3A), whereas the dynein activity on the other doublets is suppressed [8, 16–18]. The inhibition of dynein activity seems to be associated with binding of ATP to some of the four P loops of dynein, one of which is thought to be the site of ATP hydrolysis [22–24], and is overridden by the CP/radial spoke system [8, 25]. In high concentrations of Ca^{2+}, the activity of the dynein arms on doublet #3 is almost completely inhibited [8, 18, 26, 27], so that most (>90%) of the sliding is induced by the activity of dynein arms on doublet #7. In cross sections of elastase-treated axonemes, this is shown by the predominance of the 8-3 or 8-4 patterns [8], as illustrated in Figure 3A. The backward sliding induced by bending thus seems to have been caused by switching the dynein activity [8, 15–18] from doublet #7 to doublet #3 (or #4), probably mediated by the CP (Figure 3A). This interpretation hinges on the constant polarity (that is, toward the minus end of the microtubule) of force generation by the dynein arms [13, 14]. At present, however, we cannot rule out the possibility that a certain kind of dynein arm behaves as a plus end-directed motor [28], and the bending activated these arms on doublet #7.

Our previous study [8] on elastase-treated axonemes has shown that the 8-3/8-4 and 4-8 patterns, which appear under low Ca^{2+} conditions, correspond to the formation of principal (P) and reverse (R) bends, respectively (Figure 3B). These sliding patterns are thought to reflect the activity of dynein arms on doublet #7 and doublet #3, respectively. The present study has shown that the dynein arms on the rest of the doublets can also be activated by bending. In this activation, the CP may not be involved. In intact flagella, sliding does not

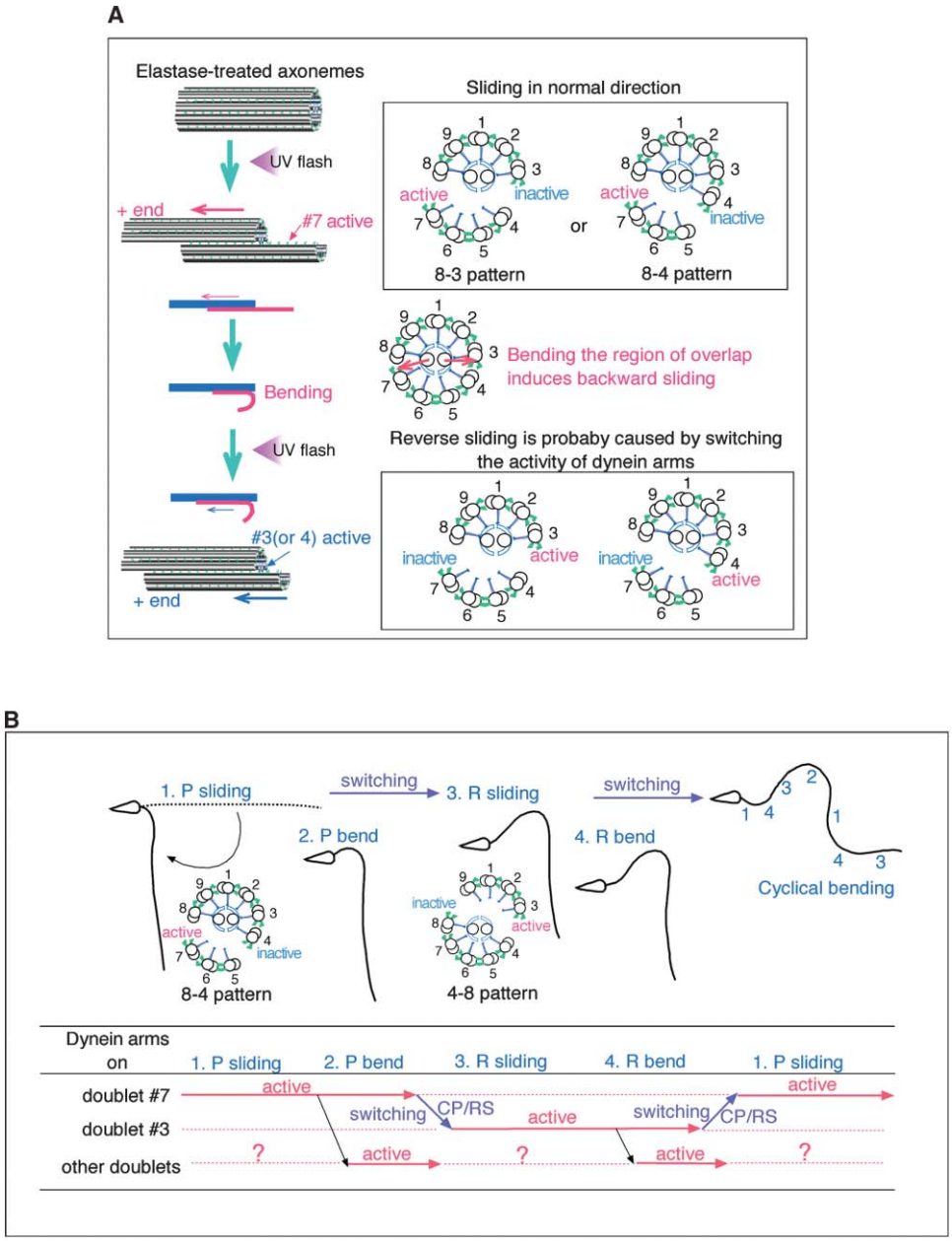

Figure 3. Selective Activation of Dynein Arms and the Direction of Sliding that Causes Bending of the Axoneme

(A) Interpretation of our results. Photoreleased ATP from caged ATP by UV flashes induced sliding disintegration of elastase-treated axonemes. Unidirectional sliding splits an elastase-treated axoneme into two microtubule bundles (8-3 or 8-4 patterns) under high Ca^{2+} conditions [8]; the sliding direction reverses after imposed bending (left diagrams). The possible sites of active dynein arms within 9 + 2 structure are indicated.

(B) A model for the self-regulatory feedback for flagellar oscillation in sea urchin spermatozoa under low Ca^{2+} conditions. It has been known that the P and R slidings induce principal and reverse (P and R) bends, respectively. Those two kinds of sliding are thought to be induced by the activity of dynein arms mainly on doublets #7 and #3 [8]. The present study has shown that, mediated by the central-pair/radial spoke system (CP/RS), bending switches the dynein activity between doublets #7 and #3. Furthermore, bending activates dynein arms on other doublets that are inactive during the P and R sliding; this type of activation of dynein is independent of the presence of CP. Coordinated dynein arm activation and inactivation, coupled with bending through the CP/RS and the doublet microtubules, is the basis for the oscillatory bending movement of flagella.

cause disintegration of the axoneme into individual doublets because of the presence of structures, such as the nexin links [29], that restrict sliding and lead to the formation of bends [11]. The growing bends may produce a force that acts transverse to the axis of the doublet microtubules in the bent region of intact flagella [5, 30]. The bending force would change the interaction, probably through radial spokes, of the CP with dynein arms in such a way that the activity of dynein arms alternates ("switches") between doublets #7 and #3. It

has recently been demonstrated in *Chlamydomonas* flagella that rotation and twisting of the CP are driven by propagating bends [31]. Twisting and rotation of the CP have also been observed in sea urchin sperm flagella, although their relationship to bend propagation is unknown [32, 33]. If the CP of sea urchin flagella behaves in a similar manner to that of *Chlamydomonas*, its rotation may well be involved in the bend-induced responses we have observed. Even so, how the CP mediates the switching of dynein activity remains elusive. The CP- and radial spoke-associated kinases and phosphatases are thought to play important roles in the transmission and transduction of regulatory signals [25]. Our findings show that the initial step of switching during each beat cycle primarily involves a mechanical effect of bending rather than chemical reactions as an essential element in the self-regulatory feedback system for oscillatory flagellar movement. How the mechanical and chemical signals interact in the regulation of flagella remains to be investigated.

Experimental Procedures

Preparation of Axonemal Fragments

Spermatozoa of the sea urchin *Pseudocentrotus depressus* were suspended in Ca^{2+}-free artificial sea water and demembranated with demembranating solution, as has been described previously [8]. The demembranation was stopped with 10 volumes of Ca^{2+}-free reactivating solution, without ATP, containing 150 mM potassium-acetate, 2 mM $MgSO_4$, 10 mM Tris-HCl (pH 8.0), 2 mM EGTA, 2% (w/v) polyethylene glycol (molecular weight 20,000), and 1 mM dithiothreitol. After demembranation, the rate of reactivation was measured by using a small portion of the demembranated axonemes, and only preparations showing >70% reactivation at 1 mM ATP were used for labeling with tetramethylrhodamine.

Demembranated axonemes were labeled with 25 μM tetramethylrhodamine (4 min on ice). The labeled sperm were pelleted at 12,000 g (3 min), resuspended in reactivating solution without ATP, and homogenized to obtain axonemal fragments. Sperm heads were removed by centrifugation at 2000 g (3 min); the supernatant containing axonemal fragments was centrifuged at 19,000 g and resuspended in reactivating solution without ATP. All procedures after demembranation were performed at 4°C or on ice.

For obtaining outer arm-depleted axonemes, labeled axonemal fragments were first treated with 0.6 M KCl solution, containing 0.6 M KCl, 2 mM $MgSO_4$, 10 mM Tris-HCl (pH 8.0), 2 mM EGTA, and 1 mM dithiothreitol, for 10 min on ice and then treated with 0.75 M KCl solution, containing 0.75 M KCl instead of 0.6 M KCl, for 60 min on ice [10].

Observation of Sliding and Application of Bending

A suspension of the axonemal fragments with the outer and inner arms or the outer arm-depleted axonemal fragments was introduced into a 15 μl perfusion chamber constructed with two glass coverslips with different sizes (25 mm × 50 mm and 9 mm ×18 mm) and 15 μm-thick plastic sheets. The smaller coverslip was placed on a larger coverslip with plastic sheets used as spacers. The axonemal fragments were treated with an elastase solution (2 μg/ml elastase [Sigma type III] and 5 μg/ml soybean trypsin inhibitor [Sigma type I-S] in reactivating solution without ATP) for 3 min at 23°C in the perfusion chamber. The elastase treatment was stopped with ovoinhibitor (50 μg/ml trypsin inhibitor from chicken egg white [Sigma type IV-O]). This was followed by perfusion with casein solution (about 1 mg/ml casein in reactivating solution without ATP) and then with reactivating solution without ATP; finally, the assay buffer was introduced into the chamber. Assay buffer contained 0.5 mM (for axonemes with the outer and inner dynein arms) or 1 mM (for outer arm-depleted axonemes) caged ATP [P^3-1-(2-nitrophenyl) ethyl ester of ATP, Dojindo Laboratories, Kumamoto, Japan], 10 units per ml hexokinase, 1% (v/v) β-mercaptoethanol, 20 mM glucose, 36 μg/ml catalase, and 216 μg/ml glucose oxidase in reactivating solution. Two kinds of reactivating solution containing different concentrations of Ca^{2+} (10^{-4} M for axonemes with the outer and inner dynein arms and Ca^{2+}-free $<10^{-9}$ M Ca^{2+} for outer arm-depleted axonemes) were used for the assay buffer because the 0.75 M KCl-treated axonemes after elastase treatment did not show sliding disintegration at high concentrations of Ca^{2+} and ATP (data not shown), indicating possible inhibition of dynein activity by Ca^{2+}, which may be independent of the regulation through the CP/radial spoke system.

Sliding disintegration was observed under an Olympus IX-70 fluorescence microscope with a ×100 objective lens (Olympus PlanApo; NA = 1.4) and an Olympus IX-RFA/CAGED attachment for photoactivation of caged ATP. Two mercury arc lamps (Ushio, USH-102D) were used for illumination. ATP was released from caged ATP by a 60 ms-UV illumination through a 360 ± 5 nm band path filter and an electronic shutter to induce sliding disintegration of the axonemes.

Axonemes were bent by a glass microneedle made with a Narishige PP-830 micropipette puller. The microneedle was attached to a Narishige MW-3 water immersion micromanipulator mounted on the microscope body. For inserting the microneedle into the assay buffer in the chamber, an open surface was obtained over the axonemes. This was done without disturbing the axonemes by first adding enough assay buffer to completely immerse the smaller (upper) coverslip and then carefully sliding "underwater" the smaller coverslip sideways. The phase-contrast image of the microneedle and the fluorescent image of axonemes could be observed simultaneously with the halogen lamp with the excitation light. When the micromanipulation was finished, the intensity of the halogen lamp was turned down, and only the image of the axonemes was recorded with an image-intensified CCD camera (Hamamatsu Photonics, C2400-87) and a videocassette recorder. Video images were captured with a computer and expressed in binary modes to analyze the sliding activity. Sliding velocities at 0.4–0.6 s or 0.9–1.1 s after a UV flash were obtained from the movement of the center of each bundle by using the NIH Image software, version 1.62 (National Institutes of Health). The sliding velocity was almost constant from about 0.3 to 1.3 s after the UV flash and then decreased gradually to zero within 2–3 s after the flash because of the presence of hexokinase in the assay buffer [12].

Supplemental Data

Supplemental Data including two videos (forward sliding and backward sliding) and a figure (illustrating the perfusion chamber with a glass microneedle) are available at http://www.current-biology.com/cgi/content/full/14/23/2113/DC1/.

Acknowledgments

We thank K. Takahashi for discussion and critical reading of the manuscript. This work was supported by a Grant-in-Aid for Scientific Research from the Japan Society for the Promotion of Science and Special Coordination Funds for Promoting Science and Technology of the Ministry of Education, Culture, Sports, Science and Technology, the Japanese Government (C.S.).

Received: August 31, 2004
Revised: September 29, 2004
Accepted: September 29, 2004
Published: December 14, 2004

References

1. Brokaw, C.J. (1989). Operation and regulation of the flagellar oscillator. In Cell Movement, Volume 1, F.D. Warner, P. Satir, and I.R. Gibbons, eds. (New York: Alan R. Liss, Inc.), pp. 267–279.
2. Shingyoji, C., Gibbons, I.R., Murakami, A., and Takahashi, K. (1991). Effect of imposed head vibration on the stability and waveform of flagellar beating in sea urchin spermatozoa. J. Exp. Biol. *156*, 63–80.
3. Shingyoji, C., Yoshimura, K., Eshel, D., Takahashi, K., and Gibbons, I.R. (1995). Effect of beat frequency on the velocity of microtubule sliding in reactivated sea urchin sperm flagella under imposed head vibration. J. Exp. Biol. *198*, 645–653.

4. Hayashibe, K., Shingyoji, C., and Kamiya, R. (1997). Induction of temporary beating in paralyzed flagella of *Chlamydomonas* mutants by application of external force. Cell Motil. Cytoskeleton *37*, 232–239.
5. Lindemann, C.B. (1994). A "Geometric Clutch" hypothesis to explain oscillations of the axoneme of cilia and flagella. J. Theor. Biol. *168*, 175–189.
6. Tani, T., and Kamimura, S. (1998). Reactivation of sea-urchin sperm flagella induced by rapid photolysis of caged ATP. J. Exp. Biol. *201*, 1493–1503.
7. Holcomb-Wygle, D.L., Schmitz, K.A., and Lindemann, C.B. (1999). Flagellar arrest behavior predicted by the geometric clutch model is confirmed experimentally by micromanipulation experiments on reactivated bull sperm. Cell Motil. Cytoskeleton *44*, 177–189.
8. Nakano, I., Kobayashi, T., Yoshimura, M., and Shingyoji, C. (2003). Central-pair-linked regulation of microtubule sliding by calcium in flagellar axonemes. J. Cell Sci. *116*, 1627–1636.
9. Yoshimura, M., and Shingyoji, C. (1999). Effects of the central pair apparatus on microtubule sliding velocity in sea urchin sperm flagella. Cell Struct. Funct. *24*, 43–54.
10. Imai, H., and Shingyoji, C. (2003). Effects of trypsin-digested outer-arm dynein fragments on the velocity of microtubule sliding in elastase-digested flagellar axonemes. Cell Struct. Funct. *28*, 71–86.
11. Shingyoji, C., and Takahashi, K. (1995). Cyclical bending movements induced locally by successive iontophoretic application of ATP to an elastase-treated flagellar axoneme. J. Cell Sci. *108*, 1359–1369.
12. Shingyoji, C., Higuchi, H., Yoshimura, M., Katayama, E., and Yanagida, T. (1998). Dynein arms are oscillating force generators. Nature *393*, 711–714.
13. Sale, W.S., and Satir, P. (1977). Direction of active sliding of microtubules in *Tetrahymena* cilia. Proc. Natl. Acad. Sci. USA *74*, 2045–2049.
14. Vale, R.D., and Toyoshima, Y.Y. (1988). Rotation and translocation of microtubules in vitro induced by dyneins from *Tetrahymena* cilia. Cell *52*, 459–469.
15. Satir, P., and Mastuoka, T. (1989). Splitting the ciliary axoneme: Implications for a "switch-point" model of dynein arm activity in ciliary motion. Cell Motil. Cytoskeleton *14*, 345–358.
16. Lindemann, C.B., Orlando, A., and Kanous, K.S. (1992). The flagellar beat of rat sperm is organized by the interaction of two functionally distinct populations of dynein bridges with a stable central axonemal partition. J. Cell Sci. *102*, 249–260.
17. Holwill, M.E.J., and Satir, P. (1994). Physical model of axonemal splitting. Cell Motil. Cytoskeleton *27*, 287–298.
18. Wargo, M.J., McPeek, M.A., and Smith, E.F. (2004). Analysis of microtubule sliding patterns in *Chlamydomonas* flagellar axonemes reveals dynein activity on specific doublet microtubules. J. Cell Sci. *117*, 2533–2544.
19. Gibbons, B.H., and Gibbons, I.R. (1973). The effect of partial extraction of dynein arms on the movement of reactivated sea-urchin sperm. J. Cell Sci. *13*, 337–357.
20. Kamiya, R., Kurimoto, E., and Muto, E. (1991). Two types of *Chlamydomonas* flagellar mutants missing different components of inner-arm dynein. J. Cell Biol. *112*, 441–447.
21. Brokaw, C.J. (1999). Computer simulation of flagellar movement: VII. Conventional but functionally different cross-bridge models for inner and outer arm dyneins can explain the effects of outer arm dynein removal. Cell Motil. Cytoskeleton *42*, 134–148.
22. Shiroguchi, K., and Toyoshima, Y.Y. (2001). Regulation of monomeric dynein activity by ATP and ADP concentrations. Cell Motil. Cytoskeleton *49*, 189–199.
23. Yagi, T. (2000). ADP-dependent microtubule translocation by flagellar inner-arm. Cell Struct. Funct. *25*, 263–267.
24. Asai, D.J., and Koonce, M.P. (2001). The dynein heavy chain: Structure, mechanics and evolution. Trends Cell Biol. *11*, 196–202.
25. Smith, E.F., and Yang, P. (2004). The radial spokes and central apparatus: Mechano-chemical transducers that regulate flagellar motility. Cell Motil. Cytoskeleton *57*, 8–17.
26. Sale, W.S. (1986). The axonemal axis and Ca^{2+}-induced asymmetry of active microtubule sliding in sea urchin sperm tails. J. Cell Biol. *102*, 2042–2052.
27. Bannai, H., Yoshimura, M., Takahashi, K., and Shingyoji, C. (2000). Calcium regulation of microtubule sliding in reactivated sea urchin sperm flagella. J. Cell Sci. *113*, 831–839.
28. Brokaw, C.J. (1997). Are motor enzymes bidirectional? Cell Motil. Cytoskeleton *38*, 115–119.
29. Summers, K.E., and Gibbons, I.R. (1973). Effects of trypsin digestion on flagellar structures and their relationship to motility. J. Cell Biol. *58*, 618–629.
30. Lindemann, C.B. (2003). Structural-functional relationships of the dynein, spokes, and central-pair projections predicted from an analysis of the forces acting within a flagellum. Biophys. J. *84*, 4115–4126.
31. Mitchell, D.R., and Nakatsugawa, M. (2004). Bend propagation drives central pair rotation in *Chlamydomonas reinhardtii* flagella. J. Cell Biol. *166*, 709–715.
32. Gibbons, I.R. (1975). The molecular basis of flagellar motility in sea urchin spermatozoa. In Molecules and Cell Movement, S. Inoué and R.E. Stephens, eds. (New York: Raven Press), pp. 207–232.
33. Omoto, C.K., Gibbons, I.R., Kamiya, R., Shingyoji, C., Takahashi, K., and Witman, G.B. (1999). Rotation of the central pair microtubules in eukaryotic flagella. Mol. Biol. Cell *10*, 1–4.